

Rapid-Response, Widely Stretchable Sensor of Aligned MWCNT/Elastomer Composites for Human Motion Detection

Katsunori Suzuki,^{*,†,‡} Koji Yataka,[†] Yasuro Okumiya,[†] Shingo Sakakibara,^{†,‡} Keisuke Sako,[§] Hidenori Mimura,[‡] and Yoku Inoue^{*,§}

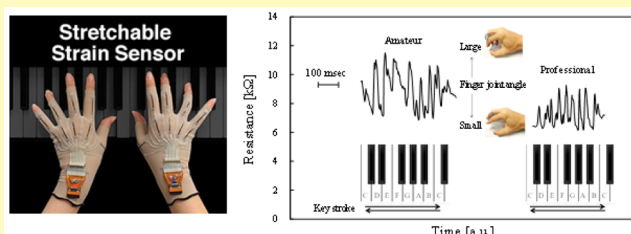
[†]Research and Development Division, Yamaha Corporation, 10-1 Nakazawa-cho, Hamamatsu, 430-8650, Japan

[‡]Research Institute of Electronics, Shizuoka University, 3-5-1 Johoku, Hamamatsu, 432-8011, Japan

[§]Department of Electronics and Materials Science, Shizuoka University, 3-5-1 Johoku, Hamamatsu, 432-8561, Japan

Supporting Information

ABSTRACT: We studied the use of carbon-nanotube-(CNT)-based strain sensors as components of a textile-based, wearable sensing system for real-time motion detection. In the stretchable sensor, millimeter-long multiwalled CNTs (MWCNTs) are unidirectionally aligned and sandwiched between elastomer layers. We synthesized urethane resin to make the elastomer, which exhibits low elasticity and an affinity for human skin. The aligned CNT layer was formed by stacking CNT webs drawn from a spinnable CNT forest. The stretchable sensor can be stretched up to 200% and exhibits a short sensing delay of less than 15 ms. The gauge factor exceeds 10, which indicates high sensitivity. Moreover, the device is thin and as soft as human skin. The demonstrated flexibility and conformable nature make this material ideally suited for wearable sensors, specifically for a textile-based, wearable, real-time, human body motion-sensing application.



KEYWORDS: strain sensor, flexible electronics, spinnable carbon nanotube, elastomer, finger motion, flexible

When piezoresistive materials are stretched by an external force, the material resistance varies to a certain extent. Therefore, when firmly attached to a deformable object without shearing or peeling, piezoresistive elements stretch as the measurement object experiences strain, resulting in variable resistance. There are two major types of strain sensors based on resistance variation: flexible sensors and stretchable sensors. The most popular of all strain sensors is a metal strain sensor called a strain gauge. It is composed of a thin electrical insulating base covered with a resistance wire grid, or a photoetched resistor foil, with lead wires attached to its edge. The strain gauge is classified as a flexible sensor. Its thin-film shape allows it to be attached to a flat or curved object surface to measure small strains of the surface of up to 5%. In contrast, a stretchable strain sensor generally consists of a composite material of polymers and conductive filler, and a variety of stretchable strain sensors composed of various material combinations exist.¹ The measurement principle underlying stretchable strain sensors differs from that of metal strain gauges; whereas a metal strain gauge detects the electric resistance variation caused by varying the geometric dimensions of its metal wires, a polymer strain sensor measures the electric resistance variation caused by structural alteration of the strained conductive paths.

Carbon materials, including carbon black (CB), graphite, single-walled carbon nanotubes (SWCNTs), and multiwalled carbon nanotubes (MWCNTs), have been used as the

composite conductive filler; fine metal particles (e.g., silver and copper) and metallic nanowires have also been used.^{2–4} Although polymer strain sensors can measure larger strains than can metal strain sensors, they are associated with several disadvantages, including low resistance variation linearity to strain, low sensitivity, and slow recovery.

New types of low-elasticity stretchable strain sensors fabricated with aligned SWCNTs and poly(dimethylsiloxane) (PDMS),⁵ MWCNT forests, polyurethane (PU),⁶ and ionic liquids and polyolefin elastomer (POE) fiber mats⁷ have recently been reported. Although these strain sensors can measure large strains exceeding the expansion/contraction ratio of 100%, further improvements in the sensor's low resistance linearity, sensitivity, and rapid response to large strains are required.

The strain value is the variation ratio relative to the initial length, as expressed in eq 1 below.

$$\epsilon = (L - L_0)/L_0 = \Delta L/L_0 \quad (1)$$

where L_0 represents the initial length, L is the elongated length, ΔL is the variation between the initial length and the elongated length, and ϵ is the strain. For instance, when the material is stretched to 200% of the initial length, the strain value is 100%.

Received: March 2, 2016

Accepted: May 18, 2016

Published: May 18, 2016

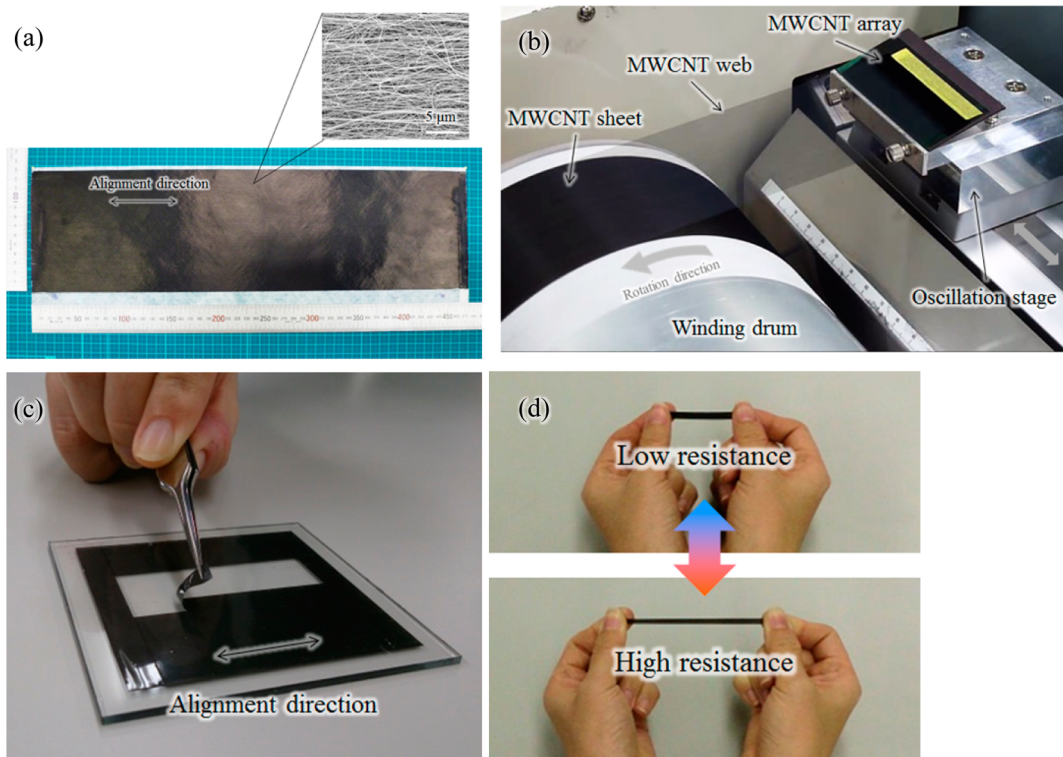


Figure 1. CNT sheet, CNT sensor, and appearance and features of a CNT strain sensor. (a) CNT sheet appearance and an image captured using a scanning electron microscope (SEM). (b) CNT web drawn from a CNT array onto a drum using the dry process. (c) Separation from the substrate. (d) CNT strain sensor exhibits thin, lightweight, and stretchable features.

The “gauge factor” (GF) represents the strain sensor sensitivity and is expressed in eq 2 below.

$$GF = \frac{\Delta R/R_0}{\Delta L/L_0} = \frac{\Delta R/R_0}{\epsilon} \quad (2)$$

where R_0 represents the initial resistance and ΔR is the variation of resistance. The higher the GF value of a sensor, the more sensitive it is. For the copper–nickel and nickel–chrome alloys generally used for metal strain gauges, the GF is approximately 2.⁸ However, the GFs of the strain sensors referred to in refs 5–7 are below 1.1, lower than those of metal strain gauges. Moreover, rapid response to large strains has not been achieved in those sensors. In terms of industrial deployment and commercialization, significant challenges remain in the manufacturing process. Although supersensitive sensors with very high GFs have been reported,^{9–16} they are not practical for sensing small strains, because excessive sensitivity causes excessive signal amplitude, requiring a wider sensing system dynamic range. Thus, both appropriate strain variation sensitivity and consistent electric circuit system sensing are required. However, no sensors satisfying all of these properties simultaneously, including linear response, wide sensing range, and rapid response to large strain, which are critical for real-time fine human motion sensing, have been developed.

Stretching sensors that detect elastomer capacitance variations have also been reported.^{17–26} The stretching sensor electrode resistance does not change when the sensor is stretched; instead, the electrodes are placed on either side of an elastomer sheet, and using the Poisson deformation of the elastomer, the change of capacitance between the electrodes associated with changes in thickness/area between them is

measured. These sensors have superior transient response and drift properties compared with resistance variation-based stretchable sensors; however, challenges remain, including the selection of an appropriate elastomer with homogeneous dielectric properties resistant to environmental variation (noise) and appropriate electrodes with resistance that remains constant even when stretched.

The novel, stretchable, MWCNT fluctuating-strain sensors (hereinafter referred to as CNT strain sensors) introduced by this work detect the resistance variation caused by a strain. These sensors can detect strains exceeding 100% and offer highly linear resistance variation relative to the strain. Additionally, their GF value is several times higher than that of metal strain gauges, corresponding to appropriately high sensitivity. These sensors offer additional attractive features, including rapid response to large strains and excellent repetition durability, i.e., robustness. Furthermore, a practical feature of the sensors is that they are highly resistant to external noises, such as changes in interconnection resistance, because resistance variation occurs in relatively high resistance ranges (from several to dozens of kilo-ohms). Moreover, the manufacturing process of these sensors is suitable for mass production, and with the wide range of possible shapes, these sensors are expected to be utilized in a large number of applications.

The CNT strain sensor is a composite structure consisting of a long, aligned MWCNT sheet (hereinafter referred to as a CNT sheet)^{27,28} and an elastomeric resin. The CNT sheet can be fabricated by dry spinning from a vertically aligned MWCNT array. Dry spinning refers to the process of successively and horizontally drawing CNTs from the edge of an MWCNT array.^{29–31} Because dry spinning allows the shape

of a macroscale material to be altered without creating dispersions, the resulting CNT sheets contain fewer impurities and offer advanced alignment properties; thus, they are becoming widely adopted as highly functional materials for various industrial applications. For instance, the Fan group (Tsinghua University) reported a stretchable conductor with constant resistance produced using the dry-spinning process.^{32,33} Additionally, CNT sheets are becoming adopted as transparent conductive films to replace indium tin oxide (ITO), which is currently widely used in the conductive films of touch-sensitive panels.^{34,35}

Following the popularization of mobile devices, wearable devices have attracted increasing interest in recent years. However, most currently available wearable devices are composed of solid devices, such as acceleration sensors, pressure sensors, and gyroscopes, which are based on microelectromechanical system (MEMS) fabrication processes. To expand wearable possibilities, such solid wearable devices are expected to be replaced by “textile-based” wearables combined with materials that are friendly to human skin, e.g., cloth and clothing.^{5,36,37} Hence, CNT strain sensors, which can adhere tightly to human surfaces and measure human motions in a noninvasive manner, are very valuable as “textile-based wearable devices.” This article aims to describe CNT strain sensor structure, operating principles, and features/characteristics and to review specific applications of “textile-based wearable devices” to monitor fine human motion.

EXPERIMENTAL SECTION

Synthesis of MWCNTs. A dry-spinnable MWCNT array was synthesized by the chloride-mediated CVD method. Iron chloride (FeCl_2) was used as a catalyst precursor, and MWCNTs (0.8 mm in height) were grown on the oxidized surface (the catalyst–supporting layer) of an Si substrate. The average diameter of the MWCNTs was 40 nm. Because the MWCNTs were very straight and superaligned, all of them were bundled while being synthesized on the substrate as a result of van der Waals forces. Therefore, when an edge of the array was drawn in a direction parallel to the substrate, the adjacent bundled MWCNTs were also drawn out from the substrate. The dry-spinning phenomenon involves this consecutive bundle detachment. This dry process transforms three-dimensional MWCNTs grown on the substrate into a two-dimensional MWCNT web network.

CNT Sheet. A CNT sheet was produced by winding and stacking a MWCNT web on a drum and cutting one end to flatten it.²⁸ A CNT sheet separated from a drum and the process of winding of an MWCNT web are represented in Figure 1a and b. The diameter of the drum used was 150 mm. The web-drawing speed was 10 mm/sec. The number of CNT web layers wound on the drum was between 8 and 12. The resistance of each CNT sheet could be adjusted by using different numbers of layers.

Elastomeric Resin. A rubber-like “elastomeric resin” with low elasticity and low-loss properties was used. For ease of bonding, durability, hydrolysis, and chemical resistance, polycarbonate-urethane resin (PCU) was chosen. For the purpose of assisting contraction, segmented polytetramethylene ether glycol-urethane (PTMGU) was used.

RESULTS AND DISCUSSION

Sensor Structure. The CNT strain sensor was manufactured by placing a CNT sheet on a flat and smooth substrate (e.g., glass) in a direction parallel to the stretching direction and impregnating it with the elastomeric resin. As indicated in Figure 1c, a CNT sensor can be formed on the substrate in any shape. The advantageous features of the CNT sensors are their high size degree of freedom, slimness, and lightweight and

stretchable nature, as shown in Figure 1d. Furthermore, urethane resin is resistant to hydrolysis in high-humidity environments. Additionally, large CNT sheets may be used for, and consequently facilitate, the transition to scaled-up mass production processes. The fracture elongation, elasticity modulus, and loss tangent ($\tan \delta$) of the CNT strain sensors were above 500%, 2–5 MPa, and less than or equal to 0.1, respectively.

Figure 2a shows the CNT sensor structure. For CNT strain sensors, the alignment direction of the CNT bundle within the

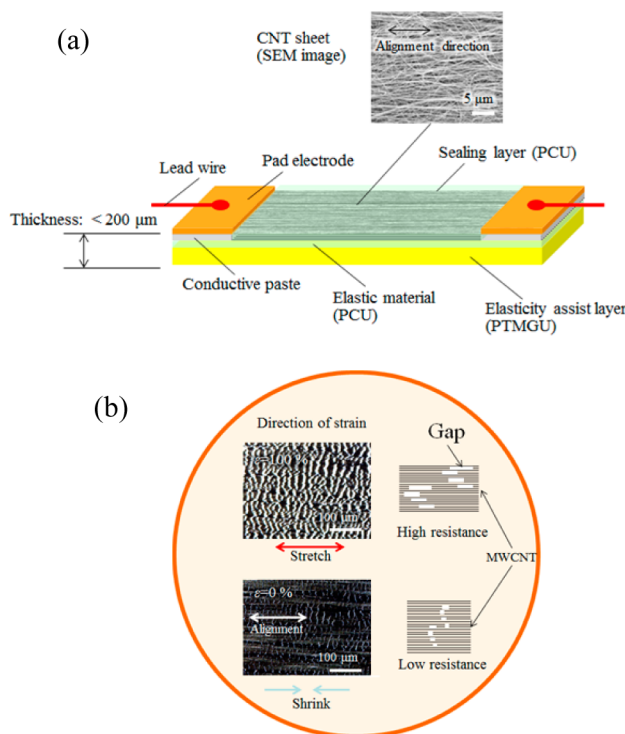


Figure 2. (a) CNT strain sensor structure. (b) Cracking of MWCNT sheet network in the CNT strain sensor; microscope image (left) and illustrated image (right).

CNT sheet and the electrode direction are consistent, and the CNT bundles, consisting of multiple CNTs, are covered and combined with an elastomer resin layer. The elastomer resin surrounding the CNT bundle was applied at a thickness of several dozen micrometers by a spin coater. To stabilize the behaviors during device contraction, an elasticity-assist layer was applied in addition to the elastomer resin surrounding the CNT bundles. The elastic modulus of the elasticity-assist layer was 2–3 MPa with a 100% modulus. The resistance increases with strain due to the cracking of the MWCNT sheet network, as shown in Figure 2b. The resistance of a CNT sheet can be adjusted by using different numbers of layers. The sensor resistance is also controllable, and this control enables the high reproducibility of the sensor devices.

Strain Sensing Characterization. Figure S1a and b show the CNT strain sensor static performance evaluation block diagram and dynamic performance evaluation block diagram, respectively. Both ends of a CNT strain sensor were clamped to a fixture, and constant current was applied to the electrodes to calculate the resistance variation from changes in output voltage caused by strains. Simultaneously, displacement signals from the linear scale were converted to strain values and were

recorded. Assuming that the CNT strain sensor has variable resistance, changes in output voltage can be expressed by the following equation.

$$V_{\text{out}} = I_{\text{set}} \times R_{\text{sensor}} \quad (3)$$

Figure 3a shows the cyclic strain-resistance characteristics of the CNT strain sensor, as measured using the above evaluation system. The CNT strain sensor used had a width of 5 mm and a gauge length of 10 mm. The displacement was 0–10 mm, i.e., strain 0–100%, and the strain acceleration was 10 mm/min. The current value was 0.5 mA, and the measurement environment temperature was maintained at 20 °C. The chart shows the results obtained over 10 consecutive elongation–contraction cycles in a stable region. The linearity of the resistance variation relative to the strain was very high. The GF value obtained via linear approximation was 10.5, indicating appropriately high sensitivity. The sensor resistance is linearly proportional to the applied tensile strain; the higher the tensile strain, the higher the sensor resistance. The detection limit of this sensor is over 200% strain.

Because of cleavage formation in the CNT bundle during the first elongation, the behavior observed in the first elongation differed from that of subsequent elongations; however, the behavior became steady after the first elongation. The inset in **Figure 3a** shows a typical hysteresis pattern. The resistance did not return to the initial value because the conductive paths decreased due to cleavage in the CNT bundle during the initial elongation. The resistance variation sensitivity is lower in the low strain range (5–10%) beginning in the second cycle. A reasonable probable cause of this decrease is the stress relaxation of the elastomeric resin; elastomeric resin does not completely recover to its initial dimensions within such a short interval. Therefore, practically, this phenomenon can be prevented by applying a pretension of at least 10% in advance. Another hysteresis behavior was also observed when the resistance sharply declined in the transition from elongation to contraction and deviated from the elongation path. A reasonable and probable reason for this behavior is that the polymer chain of the elastomeric resin under tension rapidly relaxed during the transition to the contraction range, and therefore, the internal stress of the CNT strain sensor also quickly relaxed, rapidly increasing the CNT–CNT path conductivity and decreasing the resistance.

Figure 3b shows a transient response to resistance (static characteristics). The CNT strain sensor used had a width of 3 mm and a gauge length of 10 mm. The sensor was elongated up to 10.35 mm, which corresponds to 103.5%, with an acceleration of 9.5 mm/min. The strain was then held constant for 550 s. The observed flat response is indicative of rapid resistance variation, where the decrease in resistance after the stoppage of elongation is as short as several seconds. A downward trend of resistance over long periods of time, which are generally detected in conventional filler/resin composite strain sensors, was not observed, and the fluctuation of resistance was very small.

Figure 3c and **d** show the dynamic characteristics of resistance variation relative to CNT sensor strain. The CNT strain sensor used had a width of 1.5 mm and a gauge length of 30 mm. The pretension was 16.7%. The strain was applied with a 16.7–33.3% sine wave. The frequencies were 10 and 29 Hz. The current value was 0.1 mA, and the ambient temperature was maintained at 20 °C. The result indicates that the resistance variation closely corresponded with the temporal

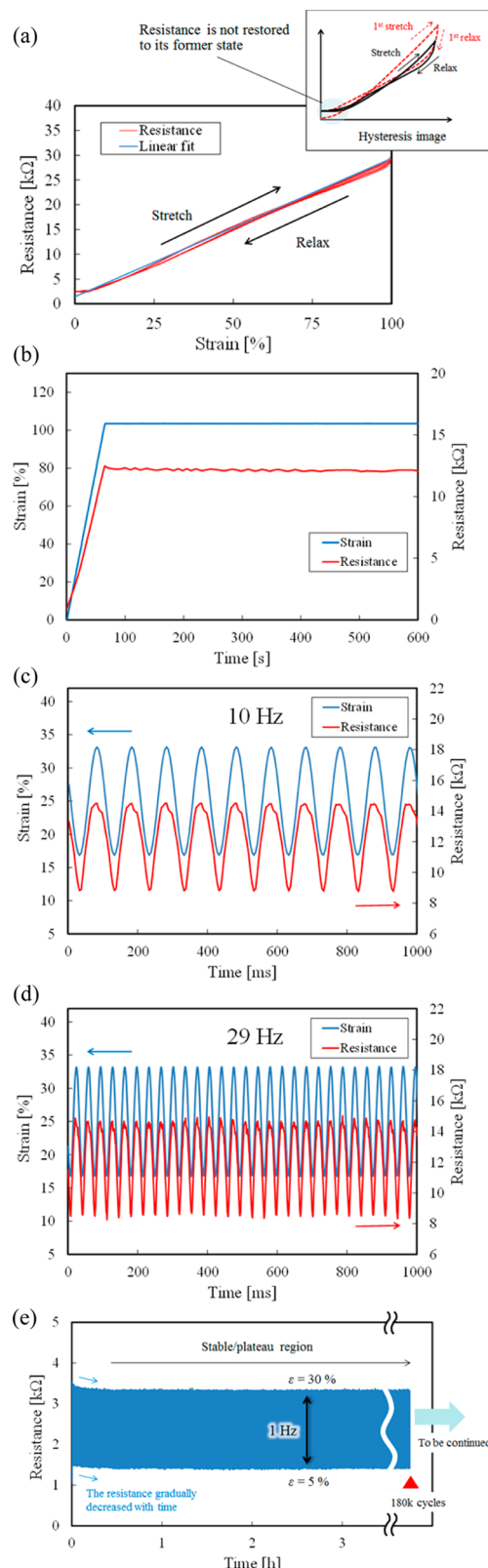


Figure 3. CNT strain sensor characteristics. (a) Cyclic strain-resistance characteristics. (b) Static characteristics. (c) Repetitions at 10 Hz. (d) Repetitions at 29 Hz. (e) Repetition durability.

changes in applied strain. Given the results described above, the CNT strain sensor exhibits an excellent rapid response. As shown in **Figure 3d**, the delay in the resistance variation was observed to be no longer than 15 ms, corresponding to

approximately half of a 29-Hz cycle (dynamic measurement movie; see Supporting Information Movie_S1).

Stability and Repeatability. Figure 3e shows the repetition durability of the CNT strain sensor. The CNT strain sensor used had a width of 3 mm and a gage length of 20 mm, and the pretension was 5%. The displacement was 1–6 mm; i.e., a repetitive strain of 5–30% was applied. The application acceleration was 10 mm/sec, i.e., 1 Hz. The current value was 0.5 mA, and the measurement environment temperature was maintained at 20 °C. As shown in Figure 3e, repetition durability over 180 000 cycles was observed. In the initial range at the start of testing, there was a slight downward trend in the resistance, but subsequently, the resistance became constant, with higher resistance variation repeatability. It is presumed that the initial resistance decline was caused by a softening of the elastomeric resin stress caused by the Mullins effect^{37,38} and a higher degree of proximity between CNTs because of internal friction. By repeated elongation and contraction, the CNT network cracks due to multiple collisions of the CNT ends, which increases the contacting surface areas between the CNTs and reduces resistance. Furthermore, the friction between the CNTs and the resin increases with increasing numbers of cracked CNTs present in the network gaps, as these increase the number of conductive paths, which leads to reduced resistance. Thus, the internal nanostructure of the CNT strain sensor and the resistance variation behavior stabilized over time. Therefore, the CNT strain sensor exhibited excellent repetition durability. The steady resistance variation behavior of the sensor over repeated CNT contact-separation cycles is rationally assumed to be partially attributable to the CNT net-like crystal structure, i.e., its bending durability (flexibility).^{39,40}

Working Mechanism. The CNT strain sensor can detect unidirectional strain by sensing a variation in the electric resistance caused by an elongation or contraction making the distance between a pair of electrodes longer or shorter (in the electrode direction), as shown in Figures 1d and 2b. Elastomeric resin elongation induces cleavage (i.e., breakage or separation) at random points in the CNT bundle. This cleavage causes gaps and increases the resistance. During contraction, rapid reorganization occurs, and the original resistance is restored. This phenomenon is repeatable. Resistance variation depends on changes in conductive paths, which are caused by physical contact between CNTs or electron transfer via the tunneling effect between CNTs in close proximity.⁴¹ Therefore, the resistance depends on the number of physical contacts between neighboring CNTs and the distance between CNTs.

Whereas the fiber length of commercially available MWCNTs is on the order of micrometers, the fiber length of the MWCNTs used in this research was 300–800 μm, which is substantially longer and prevents comparison. For such long MWCNTs, the conductive paths persist, even across the gaps created by elongation, and while the CNT strain sensor is elongating/contracting, the conductive paths slide in the longitudinal direction of the CNT fibers. A large quantity of randomly formed gaps and narrower gap intervals, which are not observed with short-fiber CNTs, short-fiber metal nanofibers, or particle or film conductive filler, are thought to underlie the high resistance variation linearity observed with respect to strain.

Figure 4a illustrates typical conductive path variations by strain amounts and an actual optical microscope image

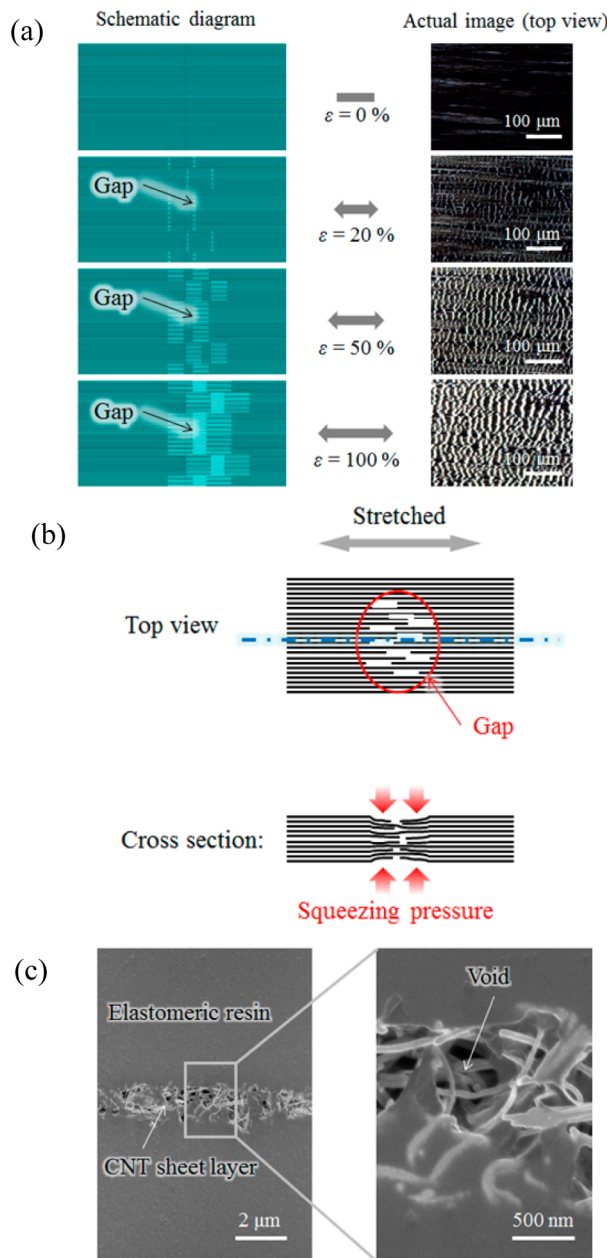


Figure 4. Typical conductive path variations by strain volumes. (a) Top view and actual image under transmitted light. (b) Cross-sectional image. (c) Cross-sectional SEM images.

obtained under transmitted light. It should be noted that most of the elongation and contraction occurs in the gaps. When the device elongates or contracts, the CNT–CNT distance in the thickness direction is changed by the internal stress and exhibits a behavior opposite that of the separation–reorganization resistance variation. During elongation, compressive stress generated by the Poisson effect is applied in the thickness direction, and the CNT–CNT distance narrows, lowering the resistance. Simultaneously, elongation increases the CNT separation, thereby increasing the resistance. In this device, however, elongation and contraction (Poisson deformation) only occur in the gaps, as shown in Figure 4b. As the numbers of CNTs in the gaps are very small, the contribution of the resistance variation caused by the internal stress to the entire resistance variation is negligible. The gap intervals are

very narrow (on the order of dozens of micrometers) and are randomly located. This is the reason why resistance varies linearly from small to large strains. In addition, the observed high sensitivity and stable repetition characteristics are also due to the porous structure resulting from CNTs not being completely covered with and/or filled by elastomeric resin. As shown in Figure 4c, voids can be observed in the CNT sheet layer. During elongation or contraction, CNT contacts inside the voids effectively act as a movable portion, which gives rise to changes in electrical resistance. This limited CNT movement also contributes to the stable changes in resistance with repetitions.

■ APPLICATION

Application Field. Current human informatics and behavioral-recognition techniques used to accurately measure human activities and biological information as well as analyze human behaviors represent active areas of research and are expected to be applied in a variety of fields, including ubiquitous networks, sports, healthcare, rehabilitation, and robotics.⁴² In fact, there are already instruments for athletes to quantify training effects and analyze dynamic motions during a game. Devices to measure and accumulate health data, such as heartbeat, activity levels, and motions, as well as services provided through smart devices, are also available to health-conscious consumers. In other words, as they become increasingly user-friendly, the applications of wearable devices are expanding to include the utilization of human biological information.^{43–45}

Because self-care is the primary basis of healthcare, particularly preventive care, devices and support systems for self-care purposes are needed. Key technologies relate to bioinstrumentation, examinations, and the analysis of accumulated hospital/clinic biological data. For these technologies, sensor systems able to constantly and easily collect biological data in noninvasive and ubiquitous manners without the need for user interventions are essential.^{5,24,46–50} The CNT strain sensor investigated herein is noninvasive and constantly wearable on the human body or on clothing, and it may repeatedly follow large motions of a human body to detect large strains with repetition durability. Thus, it could represent a novel and effective strain sensor for the purposes described above.

Currently, the predominant measurement technique used consists of motion capture imaging technologies. However, this technique has a number of disadvantages, including expensive equipment, limited measuring range because of camera light constraints, broad measuring space, and privacy issues relating to measurements in certain situations. In contrast, wearable sensor systems with CNT strain sensors have no restrictions affecting where they can be used and are capable of measuring the motions of any part of the human body for a variety of purposes. Practical advantages of CNT strain sensors include that they do not need any special circuits, e.g., amplifier circuits, and that they are resistant to external noises, such as interconnection resistance, because the resistance is highly sensitive over a relatively high resistance range. The CNT strain sensors may also detect high-frequency microvibrations at a high rate because they sense organizational changes in nanostructures; only one sensor of this type can extract advanced information, such as physical and mental human conditions, by measuring and analyzing a dynamic range of diverse biological data. Thus, these sensors are expected to be

applied in and contribute to the further development of human informatics and behavioral-recognition technologies.

Human Motion Sensing Apparel. For the future development of a practical, textile-based, wearable system integrated with CNT strain sensors, the wiring of the sensors and the electric circuit must also be stretchable. Wiring stretchability, comfort, and durability against the large strains associated with donning and removing wearable devices are essential. The authors developed a stretchable wire from silvered conductive fibers made of general synthetic fibers (e.g., polyester and nylon). Details are described in the *Supporting Information*.

The authors developed a prototype sleeve by incorporating the CNT strain sensor and the aforementioned stretchable wire into a stretchable textile, i.e., compression fabric. Figure 5a and

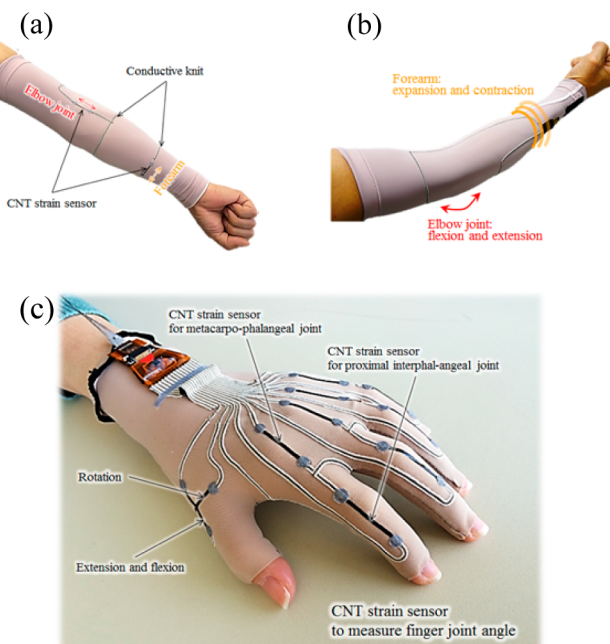


Figure 5. Sleeve with a CNT strain sensor. (a) Appearance and sensor-attachment point. (b) Working direction. (c) Data glove with CNT strain sensors.

b show the sleeve on a human arm. Human skin is very flexible; the elastic modulus and elongation rate of human skin can be as high as 1 MPa⁵¹ and 3–55%,⁵² respectively. As mentioned above, the elasticity modulus of the CNT strain sensor is 2–5 MPa. This is equivalent to or slightly higher than that of human skin, but the sensor is very thin and closely follows the motions of the human skin surface.

As indicated in Figure 5a and b, the CNT strain sensors were incorporated into the prototype sleeve in two directions: the elongation/contraction direction centered on the cubital joint and the circumferential direction of the antebrachial region. Each sensor was electrically connected to the stretchable wire end. This allows not only detection of the stretching/contracting motions of the cubital joint but also monitoring of the motions of the human body surface that were previously difficult to measure, e.g., force application on the antebrachial region based on inflation and contraction of the muscle (see *Supporting Information Movie S2*).

In conventional practice and instructional methods, it has hardly been possible to objectively evaluate body surface

conditions of athletes or dance/music instrument performers. It is widely accepted that skilled and experienced athletes/performers exhibit smooth motions, while beginners seem to exert excessive and unwanted forces in their body motions. Monitoring the force application conditions from their muscle inflation/contraction motions will help athletes/performers quantitatively comprehend their own tensions, allowing them to understand appropriate muscle tension release timing and improve their sport and dance/music performance skills. There are also various other expected applications, including respirometry based on peripheral chest/abdomen length changes caused by respiratory inflation/contraction; these changes could be measured using textile-based devices integrated with stretchable CNT sensors placed parallel to the circumferential directions of the chest/abdomen.

Data Glove. Fine motions of digital joints are often difficult to capture using imaging techniques, such as the motion capture method, because there are many blind spots. Therefore, a glove-shaped device called a “data glove” is generally used for this purpose because it is capable of detecting fine finger motions and collecting electric motion data when worn on the hand. The data glove has generated significant outcomes in various fields that require electric expression of human finger motions, such as virtual reality (VR) studies, animation and computer graphics (CG) production, and ergonomics.^{53–57}

Commercially available data gloves are designed to detect and output the “natural motions” of human hands as electric signals through variable-resistance bending sensors in film form or fiber-optic bending sensors wired along the outer surfaces of finger joints. Various improvements have been made to the gloves since their introduction to the market, and they are advertised to fit to human hands well because they are stretchable and lightweight. However, these gloves tend to feel hard and tight because of the bending sensors and hard glove fabrics, and users’ hands tend to become sweaty after long-term use; further improvements are highly desirable.

We developed prototype data gloves with less wearing burden by incorporating CNT strain sensors along the finger joint lines on a surface of thin compression fabric gloves, as shown in Figure 5c (see Supporting Information Movie S3). To evaluate these prototype data gloves, test measurements of finger motions during a piano performance requiring subtle finger movement were conducted using the data gloves. Through consultation with pianists, a compression fabric that did not disturb piano performances was selected, and the sensor length and stretchable wire layout and positions were optimized to independently detect finger motions. Finger sweatiness during a prolonged performance was also successfully eliminated by using a breathable fabric. One CNT strain sensor was provided for each metacarpophalangeal (MP) joint and proximal interphalangeal (PIP) joint of every finger to independently detect the degree of bending of each joint. When a finger joint bends, the respective CNT strain sensor elongates, and the resistance increases. When a finger joint is stretched, the sensor contracts, and the resistance decreases.

Generally speaking, professional pianists are more effortless and relaxed while performing than amateur pianists because their fingers bend less and their finger motions are smoother. Additionally, these differences have been reported to become more prominent as the performance speed increases.^{58,59} Pianist subjects wore the data gloves incorporated with CNT strain sensors, and their finger motions were measured during performances. By synchronizing and comparing the finger

motion data with the video data, the motions of each finger joint were accurately captured in real time. The results obtained from the performances of amateur and professional pianists are shown in Figure S5 using ascending and descending scales. The chart in Figure S5 shows the degree of bending of the forefinger PIP joint during performance. The results suggest that skilled pianists operate their fingers more smoothly with less finger joint bending than beginners do, which is similar to the results of reports.^{58,59} These fine finger motions (e.g., comotions/independent motions of fingers) could be analyzed, and the results could be applied to instrument performance evaluation/analysis/instruction tools and to detect finger movements in a musician’s dystonia.⁶⁰ Furthermore, various applications of the “technology to visualize finger motions” are expected in a range of fields and industries where the use of data gloves has not been possible because of their wearing burden (see Supporting Information Movie S4).

CONCLUSION

In this article, a uniquely stretchable strain sensor composed of a long, aligned MWCNT sheet and elastomeric resin was introduced. The sensor is not only capable of statically and dynamically detecting large strains but is also thin, lightweight, and easily formed into various shapes. This suggests the possible creation of both wearable systems and services with unprecedented values by incorporating the sensor into objects that are not compatible with conventional sensing devices, e.g., objects with complex shapes and biological surfaces.

ASSOCIATED CONTENT

S Supporting Information

The Supporting Information is available free of charge on the ACS Publications website at DOI: [10.1021/acssensors.6b00145](https://doi.org/10.1021/acssensors.6b00145).

Data collection; CNT strain sensor performance evaluation block diagrams; Stretchable wire, enlarged view and appearance of conductive stretchable wire; Conductive stretchable wire performance; Multipole wiring of the stretchable wire onto a flexible printed circuit; The time-varying waveforms of the angles at the proximal-interphalangeal (PIP) joints of the index finger of a pianist ([PDF](#))

Dynamic measurement of the CNT strain sensors ([MPG](#))

Human motion sensing apparel performance of the prototype sleeve ([MPG](#))

Computer graphics of finger motion captured by the prototype data glove ([MPG](#))

Test measurements of finger motions during a piano performance with the prototype data gloves ([MPG](#))

AUTHOR INFORMATION

Corresponding Authors

*E-mail: katsunori.suzuki@music.yamaha.com.

*E-mail: inoue.yoku@shizuoka.ac.jp.

Notes

The authors declare no competing financial interest.

REFERENCES

- (1) Hu, B.; Chen, W.; Zhou, J. High Performance Flexible Sensor Based on Inorganic Nanomaterials. *Sens. Actuators, B* **2013**, *176*, 522–533.

- (2) Zou, J.-F.; Yu, Z.-Z.; Pan, Y.-X.; Fang, X.-P.; Ou, Y.-C. Conductive Mechanism of Polymer/Graphite Conducting Composites with Low Percolation Threshold. *J. Polym. Sci., Part B: Polym. Phys.* **2002**, *40*, 954–963.
- (3) Luheng, W.; Tianhuai, D.; Peng, W. Thin Flexible Pressure Sensor Array based on Carbon Black/Silicone Rubber Nanocomposite. *IEEE Sens. J.* **2009**, *9*, 1130–1135.
- (4) Yasuoka, T.; Shimamura, Y.; Todoroki, A. Patch-Type Large Strain Sensor Using Elastomeric Composite Filled with Carbon Nanofibers. *Int. J. Aeronaut. Space Sci.* **2013**, *14*, 146–151.
- (5) Yamada, T.; Hayamizu, Y.; Yamamoto, Y.; Yomogida, Y.; Izadi-Najafabadi, A.; Futaba, D. N.; Hata, K. A Stretchable Carbon Nanotube Strain Sensor for Human-Motion Detection. *Nat. Nanotechnol.* **2011**, *6*, 296–301.
- (6) Shin, M. K.; Oh, J.; Lima, M.; Kozlov, M. E.; Kim, S. J.; Baughman, R. H. Elastomeric Conductive Composites based on Carbon Nanotube Forests. *Adv. Mater.* **2010**, *22*, 2663–2667.
- (7) Ma, Z.; Su, B.; Gong, S.; Wang, Y.; Yap, L. W.; Simon, G. P.; Cheng, W. Liquid-Wetting-Solid Strategy to Fabricate Stretchable Sensors for Human-Motion Detection. *ACS Sens.* **2016**, *1*, 303.
- (8) Arshak, K.; Perrem, R. Fabrication of a Thin-Film Strain-Gauge Transducer Using $\text{Bi}_2\text{O}_3\text{-V}_2\text{O}_5$. *Sens. Actuators, A* **1993**, *36*, 73–76.
- (9) Sobha, A.; Narayankutty, S. K. Improved Strain Sensing Property of Functionalised Multiwalled Carbon Nanotube/Polyaniline Composites in TPU Matrix. *Sens. Actuators, A* **2015**, *233*, 98–107.
- (10) Liao, X.; Liao, Q.; Yan, X.; Liang, Q.; Si, H.; Li, M.; Wu, H.; Cao, S.; Zhang, Y. Flexible and Highly Sensitive Strain Sensors Fabricated by Pencil Drawn for Wearable Monitor. *Adv. Funct. Mater.* **2015**, *25*, 2395–2401.
- (11) Rahimi, R.; Ochoa, M.; Yu, W.; Ziaie, B. Highly Stretchable and Sensitive Unidirectional Strain Sensor via Laser Carbonization. *ACS Appl. Mater. Interfaces* **2015**, *7*, 4463–4470.
- (12) Soltanian, S.; Servati, A.; Rahamanian, R.; Ko, F.; Servati, P. Highly Piezoresistive Compliant Nanofibrous Sensors for Tactile and Epidermal Electronic Applications. *J. Mater. Res.* **2015**, *30*, 121–129.
- (13) Kost, J.; Narkis, M.; Fouix, A. Effects of Axial Stretching on the Resistivity of Carbon Black Filled Silicone Rubber. *Polym. Eng. Sci.* **1983**, *23*, 567–571.
- (14) Zhou, J.; Gu, Y.; Fei, P.; Mai, W.; Gao, Y.; Yang, R.; Bao, G.; Wang, Z. L. Flexible Piezotronic Strain Sensor. *Nano Lett.* **2008**, *8*, 3035–3040.
- (15) Wang, X.; Fu, X.; Chung, D. D. L. Strain Sensing Using Carbon Fiber. *J. Mater. Res.* **1999**, *14*, 790–802.
- (16) Anand, S. V.; Mahapatra, D. R. Quasi-Static and Dynamic Strain Sensing Using Carbon Nanotube/Epoxy Nanocomposite Thin Films. *Smart Mater. Struct.* **2009**, *18*, 045013.
- (17) Cotton, D. P. J.; Graz, I. M.; Lacour, S. P. A Multifunctional Capacitive Sensor for Stretchable Electronic Skins. *IEEE Sens. J.* **2009**, *9*, 2008–2009.
- (18) Rosset, S.; O'Brien, B. M.; Gisby, T.; Xu, D.; Shea, H. R.; Anderson, I. A. In *Tunable Grating with Active Feedback*; Bar-Cohen, Y., Ed.; Proc. SPIE: Bellingham, WA, 2013; pp 86872F–86872F–86811.
- (19) O'Brien, B.; Gisby, T.; Anderson, I. A. In *Stretch Sensors for Human Body Motion*; Bar-Cohen, Y., Ed.; Proc. SPIE: SPIE: Bellingham, WA, 2014; pp 90S618–90S618–90S619.
- (20) Cohen, D. J.; Mitra, D.; Peterson, K.; Maharbiz, M. M. A Highly Elastic, Capacitive Strain Gauge based on Percolating Nanotube Networks. *Nano Lett.* **2012**, *12*, 1821–1825.
- (21) Cai, L.; Song, L.; Luan, P.; Zhang, Q.; Zhang, N.; Gao, Q.; Zhao, D.; Zhang, X.; Tu, M.; Yang, F.; Zhou, W.; Fan, Q.; Luo, J.; Zhou, W.; Ajayan, P. M.; Xie, S. Super-Stretchable, Transparent Carbon Nanotube-Based Capacitive Strain Sensors for Human Motion Detection. *Sci. Rep.* **2013**, *3*, 3048.
- (22) Lipomi, D. J.; Vosgueritchian, M.; Tee, B. C. K.; Hellstrom, S. L.; Lee, J. A.; Fox, C. H.; Bao, Z. Skin-Like Pressure and Strain Sensors based on Transparent Elastic Films of Carbon Nanotubes. *Nat. Nanotechnol.* **2011**, *6*, 788–792.
- (23) Xu, F.; Zhu, Y. Highly Conductive and Stretchable Silver Nanowire Conductors. *Adv. Mater.* **2012**, *24*, 5117–5122.
- (24) Yao, S.; Zhu, Y. Wearable Multifunctional Sensors Using Printed Stretchable Conductors Made of Silver Nanowires. *Nanoscale* **2014**, *6*, 2345–2352.
- (25) Hu, W.; Niu, X.; Zhao, R.; Pei, Q. Elastomeric Transparent Capacitive Sensors based on an Interpenetrating Composite of Silver Nanowires and Polyurethane. *Appl. Phys. Lett.* **2013**, *102*, 083303.
- (26) Hammock, M. L.; Chortos, A.; Tee, B. C.; Tok, J. B.; Bao, Z. 25th Anniversary Article: The Evolution of Electronic Skin (E-Skin): A Brief History, Design Considerations, and Recent Progress. *Adv. Mater.* **2013**, *25*, 5997–6038.
- (27) Inoue, Y.; Kakihata, K.; Hiroto, Y.; Horie, T.; Ishida, A.; Mimura, H. One-Step Grown Aligned Bulk Carbon Nanotubes by Chloride Mediated Chemical Vapor Deposition. *Appl. Phys. Lett.* **2008**, *92*, 213113.
- (28) Inoue, Y.; Suzuki, Y.; Minami, Y.; Muramatsu, J.; Shimamura, Y.; Suzuki, K.; Ghemes, A.; Okada, M.; Sakakibara, S.; Mimura, H. Anisotropic Carbon Nanotube Papers Fabricated from Multiwalled Carbon Nanotube Webs. *Carbon* **2011**, *49*, 2437–2443.
- (29) Jiang, K.; Li, Q.; Fan, S. Nanotechnology: Spinning Continuous Carbon Nanotube Yarns. *Nature* **2002**, *419*, 801.
- (30) Jiang, K.; Wang, J.; Li, Q.; Liu, L.; Liu, C.; Fan, S. Superaligned Carbon Nanotube Arrays, Films, and Yarns: A Road to Applications. *Adv. Mater.* **2011**, *23*, 1154–1161.
- (31) Zhang, M.; Atkinson, K. R.; Baughman, R. H. Multifunctional Carbon Nanotube Yarns by Downsizing an Ancient Technology. *Science* **2004**, *306*, 1358–1361.
- (32) Feng, C.; Liu, K.; Wu, J.-S.; Liu, L.; Cheng, J.-S.; Zhang, Y.; Sun, Y.; Li, Q.; Fan, S.; Jiang, K. Flexible, Stretchable, Transparent Conducting Films Made from Superaligned Carbon Nanotubes. *Adv. Funct. Mater.* **2010**, *20*, 885–891.
- (33) Yu, Y.; Luo, S.; Sun, L.; Wu, Y.; Jiang, K.; Li, Q.; Wang, J.; Fan, S. Ultra-Stretchable Conductors based on Buckled Super-Aligned Carbon Nanotube Films. *Nanoscale* **2015**, *7*, 10178–10185.
- (34) Liu, K.; Sun, Y.; Liu, P.; Lin, X.; Fan, S.; Jiang, K. Cross-Stacked Superaligned Carbon Nanotube Films for Transparent and Stretchable Conductors. *Adv. Funct. Mater.* **2011**, *21*, 2721–2728.
- (35) Fu, W.; Liu, L.; Jiang, K.; Li, Q.; Fan, S. Super-Aligned Carbon Nanotube Films as Aligning Layers and Transparent Electrodes for Liquid Crystal Displays. *Carbon* **2010**, *48*, 1876–1879.
- (36) De Rossi, D.; Della Santa, A.; Mazzoldi, A. Dressware: Wearable Hardware. *Mater. Sci. Eng., C* **1999**, *7*, 31–35.
- (37) Segev-Bar, M.; Haick, H. Flexible Sensors based on Nanoparticles. *ACS Nano* **2013**, *7*, 8366–8378.
- (38) Junisbekov, T. M.; Kestel'man, V. N.; Malinin, N. I. *Stress Relaxation in Viscoelastic Materials*; Science Publishers: Enfield, NH, 2003.
- (39) Demczyk, B. G.; Wang, Y. M.; Cumings, J.; Hetman, M.; Han, W.; Zettl, A.; Ritchie, R. O. Direct Mechanical Measurement of the Tensile Strength and Elastic Modulus of Multiwalled Carbon Nanotubes. *Mater. Sci. Eng., A* **2002**, *334*, 173–178.
- (40) Hayashi, T.; O'Connor, T. C.; Higashiyama, K.; Nishi, K.; Fujisawa, K.; Muramatsu, H.; Kim, Y. A.; Sumpter, B. G.; Meunier, V.; Terrones, M.; Endo, M. A Reversible Strain-Induced Electrical Conductivity in Cup-Stacked Carbon Nanotubes. *Nanoscale* **2013**, *5*, 10212–10218.
- (41) Sheng, P.; Sichel, E. K.; Gittleman, J. I. Fluctuation-Induced Tunneling Conduction in Carbon-Polyvinylchloride Composites. *Phys. Rev. Lett.* **1978**, *40*, 1197–1200.
- (42) Choudhury, T.; Consolvo, S.; Harrison, B.; Hightower, J.; Lamarca, A.; LeGrand, L.; Rahimi, A.; Rea, A.; Bordello, G.; Hemingway, B. The Mobile Sensing Platform: An Embedded Activity Recognition System. *IEEE Pervasive Comput.* **2008**, *7*, 32–41.
- (43) Lara, O. D.; Labrador, M. A. A Survey on Human Activity Recognition Using Wearable Sensors. *IEEE Commun. Surv. Tutorials* **2013**, *15*, 1192–1209.

- (44) Custodio, V.; Herrera, F. J.; Lopez, G.; Moreno, J. I. A Review on Architectures and Communications Technologies for Wearable Health-Monitoring Systems. *Sensors* **2012**, *12*, 13907–13946.
- (45) Pantelopoulos, A.; Bourbakis, N. G. A Survey on Wearable Sensor-Based Systems for Health Monitoring and Prognosis. *IEEE Trans. Syst. Man. Cybern. C Appl. Rev.* **2010**, *40*, 1–12.
- (46) Burns, A.; Greene, B. R.; McGrath, M. J.; O'Shea, T. J.; Kuris, B.; Ayer, S. M.; Stroiescu, F.; Cionca, V. Shimmer—a Wireless Sensor Platform for Noninvasive Biomedical Research. *IEEE Sens. J.* **2010**, *10*, 1527–1534.
- (47) Lu, N.; Kim, D.-H. Flexible and Stretchable Electronics Paving the Way for Soft Robotics. *Robotics* **2013**, *1*, 53–62.
- (48) Lu, N.; Lu, C.; Yang, S.; Rogers, J. Highly Sensitive Skin-Mountable Strain Gauges Based Entirely on Elastomers. *Adv. Funct. Mater.* **2012**, *22*, 4044–4050.
- (49) Godfrey, A.; Conway, R.; Meagher, D.; O'Loughlin, G. Direct Measurement of Human Movement by Accelerometry. *Med. Eng. Phys.* **2008**, *30*, 1364–1386.
- (50) Kim, D. H.; Ghaffari, R.; Lu, N.; Rogers, J. A. Flexible and Stretchable Electronics for Biointegrated Devices. *Annu. Rev. Biomed. Eng.* **2012**, *14*, 113–128.
- (51) Agache, P. G.; Monneur, C.; Leveque, J. L.; De Rigal, J. Mechanical Properties and Young's Modulus of Human Skin in Vivo. *Arch. Dermatol. Res.* **1980**, *269*, 221–232.
- (52) Street, R. A.; Arias, A. C. In *Stretchable Electronics*; Someya, T., Ed.; Wiley-VCH Verlag GmbH & Co., KGaA: Weinheim, Germany, 2012; pp 355–378.
- (53) Bates, J. Virtual Reality, Art, and Entertainment. *Presence Teleoperators Virtual Environ.* **1992**, *1*, 133–138.
- (54) Blake, J.; Gurocak, H. B. Haptic Glove with Mr Brakes for Virtual Reality. *Mechatronics, IEEE/ASME Transactions on* **2009**, *14*, 606–615.
- (55) Xu, D. Proc. *IEEE 18th International Conference on Pattern Recognition*, Los Alamitos, CA; Tang, Y. Y.; Wang, S. P.; Lorette, G.; Yeung, D.S.; Yan, H., Eds.; IEEE Computer Society: Washington, DC, 2006; p 519.
- (56) Wang, R. Y.; Popović, J. Real-Time Hand-Tracking with a Color Glove. *ACM Trans. Graph.* **2009**, *28*, 63.
- (57) Mitobe, K.; Kaiga, T.; Yukawa, T.; Miura, T.; Tamamoto, H.; Rodgers, A.; Yoshimura, N. Development of a Motion Capture System for a Hand Using a Magnetic Three Dimensional Position Sensor. In *ACM SIGGRAPH 2006 Research Posters*; ACM: Boston, MA, 2006; p 102.
- (58) Furuya, S.; Altenmüller, E. Flexibility of Movement Organization in Piano Performance. *Front. Hum. Neurosci.* **2013**, *7*, 173.
- (59) Furuya, S.; Flanders, M.; Soechting, J. F. Hand Kinematics of Piano Playing. *J. Neurophysiol.* **2011**, *106*, 2849–2864.
- (60) Furuya, S.; Tominaga, K.; Miyazaki, F.; Altenmüller, E. Losing Dexterity: Patterns of Impaired Coordination of Finger Movements in Musician's Dystonia. *Sci. Rep.* **2015**, *5*, 13360.